Binaries Among Debris Disk Stars: IRAS vs Spitzer

David R. Rodriguez and Ben Zuckerman

University of California, Los Angeles, CA 90095

ABSTRACT

We have gathered a sample of 113 main-sequence stars (ages older than 10 Myr) with known infrared excesses. Our sample includes stars within 100 pc and ranges from spectral types B8 to K2, though most (89) are A or F stars. Most of these excesses were discovered with IRAS and many have been confirmed with MIPS on Spitzer. We are collecting published information and making our own measurements on these stars to determine if they are binaries or multiple star systems. With this we will obtain a measure of how often binary stars contain debris disks and determine whether properties such as the average dust temperature or L_{IR}/L_* are sensitive to the presence of companions. This work will be compared with the Trilling et al. (2007) Spitzer-based study of debris disks in main-sequence binary systems.

Subject headings: binaries: general — infrared: stars — planetary systems: formation

1. Introduction

Many stars are known to have infrared excesses, which are due to the presence of dusty disks surrounding the star. These disks can be primordial with gas and dust from the star formation process or debris disks formed later on as a result of collisions between rocky planetesimals (Zuckerman 2001). Many stars are also known to be binaries. For example, Duquennoy & Mayor (1991) estimate that 57% of G stars may be multiple systems. A question naturally arises: if many stars are in multiple systems, what does this say about the formation and evolution of disks and planets?

There has been some previous effort to address this issue. Trilling et al. (2007) used Spitzer MIPS to search for infrared excess among 69 known binary systems. They not only found that some binary systems have debris disks, but also that that the incidence of debris disks among binaries is marginally higher than for single AFGK stars older than 600 Myr.

We describe our sample in §2 and our procedure in §3. The subsequent sections (§4-7) describe our results concerning ages, fractional luminosties, dust temperatures, and binary separations. Our conclusions are summarized in §8.

2. Sample

We have approached the question of multiplicity among debris disk systems from a different direction than Trilling et al. (2007). We have selected a sample of stars with known infrared excesses that satisfy several criteria: ages older than 10 million years (to reduce the chances that we include protoplanetary disks) and distances within 100 parsecs (to ensure we have sufficient information). We constructed our sample from Rhee et al. (2007), Rebull et al. (2008), Chen et al. (2005), and included BD+20 307 from Song et al. (2005).

For the IRAS sample from Rhee et al. (2007), we only selected objects that were not new IR-excess stars (unless they had confirmation with Spitzer). Many Spitzer studies tend to be biased against binaries, so we were careful to select samples that were not biased in favor or against binaries. The Rebull et al. (2008) study was based on stars in the Beta Pictoris moving group while Chen et al. (2005) searched for debris disks among nearby, young stars.

From these references we obtain stellar properties such as spectral type, age, fractional luminosity, dust temperature, and dust orbital semi-major axis. The dust properties were derived from blackbody fits to the excess emission after modeling the stellar photosphere.

This resulted in a catalog of 113 systems with spectral types B8 to K2 (see Fig 1). The majority of these stars are IRAS detections from Rhee et al. (2007). Many, though, have been confirmed by Spitzer. Two of our objects overlap with the Trilling et al. (2007) sample: HIP 15197 and HIP 66704.

3. Procedure

After specifying our sample, we performed a literature search to determine which of our stars are known to be multiples. We found 43 binary or multiple star systems within our sample. This corresponds to a multiplicity of $37^{+5}_{-4}\%$, where the errors are binomial errors estimated as described by Burgasser et al. (2003). We have broken down our sample by spectral type in Table 1, where we have also included the multiple fraction obtained by Eggleton & Tokovinin (2008, from now on ET08) and Duquennoy & Mayor (1991).

For some of our targets, very little literature data was available, especially concerning searches for companions. This leads us to believe that we may be missing some binaries or multiples in our sample.

4. Ages

We have compared our single and multiple sample based on the distribution by age. Our ages come mostly from the main reference where we found the given star with the exception being Algol

for which we use 300 Myr (Su et al. 2006). The distribution is shown in Fig 2. The fractions are the number of single stars in that age bin over the total number of single stars and, similarly, for the multiple star sample. The Trilling et al. (2007) conclusion of higher fraction of excesses in binaries was for stars of ages 600 Myr or higher. Our sample of 600 Myr and older stars has 6 single stars (8% of all single stars) and 13 multiple stars (31% of all multiples). Our > 600 Myr subsample suggests that 68^{+8}_{-12}% of debris disk stars 600 Myr or older are binaries, with the large uncertainties due to small number statistics.

5. Fractional Luminosities

Fractional luminosity (L_{IR}/L_*) is the ratio of the excess infrared luminosity to the total energy output from the star. In Fig 3, we plot the distribution of our single and multiple stars with respect to fractional luminosities and compare it to Trilling et al. (2007). The single stars tend to have higher fractional luminosities than the multiple stars. The majority of Trilling's fractional luminosities are determined by using a blackbody that fits a 70μm excess and the 3σ upper limit on 24μm emission. This procedure results in the maximum possible values for L_{IR}/L_* so these can be considered upper limits. Several stars from Chen et al. (2005) and Rebull et al. (2008) had detections only at 70μm but the temperatures were set at around 40K (see discussion in §6). We have scaled the L_{IR}/L_* values given in Chen et al. (2005) and Rebull et al. (2008) as $L_{IR}/L_* \propto T$ in order to determine fractional luminosities consistent with our chosen temperature of 73K.

The Kolmogorov-Smirnov (KS) test finds all three distributions to be different from one another at the 99% significance level. The KS test probabilities are 3.80E-3 for single vs multiple, 1.57E-8 for single vs Trilling, and 4.58E-3 for multiple vs Trilling. This suggests that there may be difference in the L_{IR}/L_* distribution based on multiplicity in that multiple stars have lower fractional luminosities.

To address this difference in fractional luminosity we compare L_{IR}/L_* with age. Previous studies (for example, Rhee et al. (2007)) have found that the fractional luminosity diminishes with increasing age. Figure 4 is a plot of L_{IR}/L_* vs. age for our sample. Both single and multiple stars have L_{IR}/L_* decrease with age. The distribution of points looks very similar for both, but the multiple stars tend to be older (see §4).

Figure 5 shows a similar plot, but with averaged L_{IR}/L_* for a set of age bins. The age bins have been selected so that there are enough objects in that bin for a statistically significant average. Our choice of bins have about 10-25% of the objects in them (however, the last two single star bins have only 8% and 4%, respectively). The same trend of decreasing L_{IR}/L_* vs. age can be seen, though it seems to flatten out at for the older age bins. BD+20 307 has an unusually high L_{IR}/L_* (4%) so we have included two multiple data points on the oldest age bin. The highest one includes BD+20 307 while the lower one (in yellow) does not. Although there is a spread (see Fig 4), the multiples (without BD+20 307) have average L_{IR}/L_* lower than single stars for all ages.

6. Dust Temperatures

In Fig 6, we plot the dust temperature distribution in our sample and Trilling's. For objects with only an excess at 60μm, Rhee et al. (2007) assigned a temperature of 85K so that the blackbody peaks at that wavelength. This is the reason why the peak at 81-90K is higher than the others.

For objects with excess emission only at 70μm, Rebull et al. (2008) set a temperature of 41K corresponding to the peak for λF_λ while Chen et al. (2005) uses a temperature of 40K, based on a modified blackbody fit to the dust around AU Mic. Most of our data come from Rhee et al. (2007) which use νF_ν so we have set the temperature for those objects in Chen et al. (2005) and Rebull et al. (2008) with only 70μm excesses to be 73K. In comparison, Trilling et al. (2007) determine upper limits on temperature by using the 3σ upper limit on the 24μm emission for those objects with only 70μm excesses.

The KS test shows no statistical difference between our single and multiple systems (p=0.28). It does show a difference between both samples and Trilling's, in the sense that the latter temperatures are larger, with probabilities of 2.23E-7 and 5.13E-5 for Trilling against single and multiples, respectively.

7. Separations

We have also searched for the separations of our binary/multiple stars and have obtained data for 32 of our 42 systems. Tables 2 and 3 list our separations for the binary and multiple stars. Our separations come from Hoffleit & Warren (1995); ESA (1997); Worley & Douglass (1997); Tokovinin (1997); Alzner (1998); Pourbaix (2000); Fabricius et al. (2002); and Dommanget & Nys (2002).

We compute the ratio of the blackbody dust orbital semi-major axis to binary separation for 32 of our stars. As discussed in §6, we have modified the temperatures for a few of our objects. To be consistent we have also modified the respective dust semi-major axis by scaling as $R \propto T^{-2}$. Twenty-one of these 32 stars have only one companion (ie, they are binary) while the remaining have more than one. For these multiple star systems we have used only the smallest of the separations. We assume that the dust is present around the primary star in the system.

In Fig 7 we have binned them according to whether this ratio is < 0.15, between 0.15 and 3.5, or > 3.5. The dividing lines between the three bins correspond to approximately where the dust enters or exits from unstable regions (Trilling et al. 2007). For values less than 0.15 we have stable circumstellar disks while for values larger than 3.5 we have stable circumbinary disks. It can clearly be seen that while Trilling's sample consists mostly of circumbinary disks, ours is made up of mostly circumstellar disks.

In Fig 8 we plot the distance ratio against Log L_{IR}/L_*. We again see that most of our objects lie towards the lower ratios, however, our sample has a wider range of L_{IR}/L_* than Trilling's

sample. In Fig 9 we plot the dust semi-major axis against the binary separation. It is evident that we are missing many close binaries. Measurements of radial velocities or searches with adaptive optics imaging may find these missing binary systems.

8. Conclusions

We find that the fraction of stars in binary or multiple systems among our debris disk systems is $37^{+5}_{-4}\%$. This is less than the anticipated $\sim 1/2$ of stars and could be due to incomplete multiplicity data for some of our stars. Based on our distribution of systems by star separation, it is likely that we are missing close binary systems with circumbinary disks. Radial velocity or adaptive optics searches may help us find these missing binaries.

Our stars tend to be younger than those in Trilling et al. (2007), but the multiplicity fraction in old IRAS star systems (>600 Myr) is $68^{+8}_{-12}\%$. Subject to the caveat of small number statistics, this suggests that for old systems, binary or multiple star systems are more likely than single stars to contain debris disks. Our multiples tend to have lower fractional luminosities than single stars, however, this may be a result of our multiple stars being older than single stars. The distribution of dust temperatures is similar for both single and binary/multiple stars.

REFERENCES

Alzner, A. 1998, A&AS, 132, 237

Burgasser, A.J., Kirkpatrick, J.D., Reid, I.N., Brown, M.E., Miskey, C.L., & Gizis, J.E. 2003, ApJ, 586, 512

Chen, C.H., et al. 2005, ApJ, 634, 1372

Dommanget, J., & Nys, O. 2002, VizieR Online Data Catalog, 1274, 0

Duquennoy, A., & Mayor, M. 1991, A&A, 248, 485

Eggleton, P.P., & Tokovinin, A.A. 2008, MNRAS, 389, 869

Hoffleit, D., & Warren, W. H., Jr. 1995, VizieR Online Data Catalog, 5050, 0

ESA 1997, VizieR Online Data Catalog, 1239, 0

Fabricius, C., Høg, E., Makarov, V. V., Mason, B. D., Wycoff, G. L., & Urban, S. E. 2002, A&A, 384, 180

Pourbaix, D. 2000, A&AS, 145, 215

Tokovinin, A. A. 1997, A&AS, 124, 75

Trilling, D.E., et al. 2007, ApJ, 658, 1289

Rhee, J.H., Song, I., Zuckerman, B., & McElwain, M. 2007, ApJ, 660, 1556

Rebull, L.M., et al. 2008, ApJ, 681, 1484

Song, I., Zuckerman, B., Weinberger, A.J., & Becklin, E.E. 2005, Nature, 436, 363

Su et al. 2006, ApJ, 653, 675

Worley, C. E., & Douglass, G. G. 1997, A&AS, 125, 523

Zuckerman, B. 2001, ARA&A, 39, 549

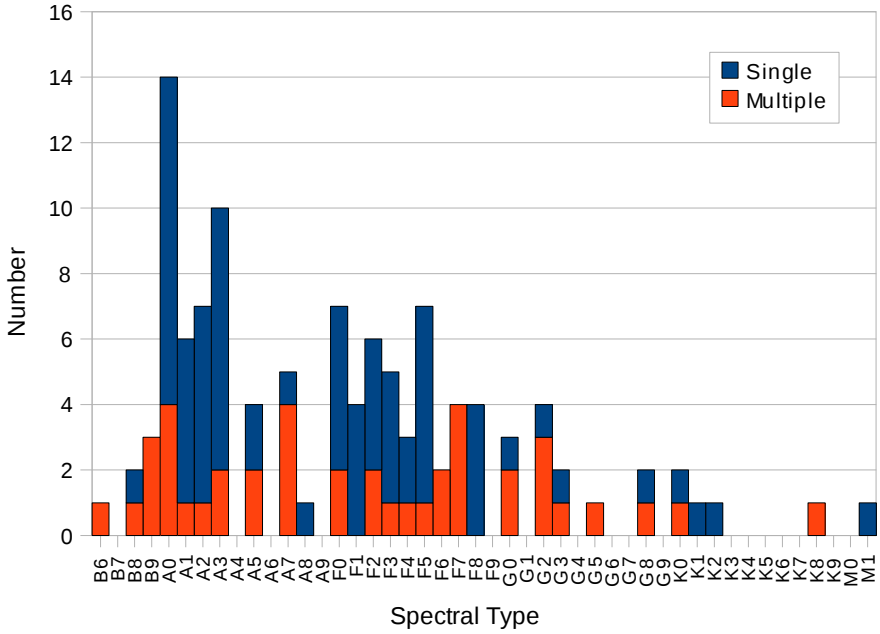

Fig. 1.— Histogram of star's spectral types (from SIMBAD or main reference).

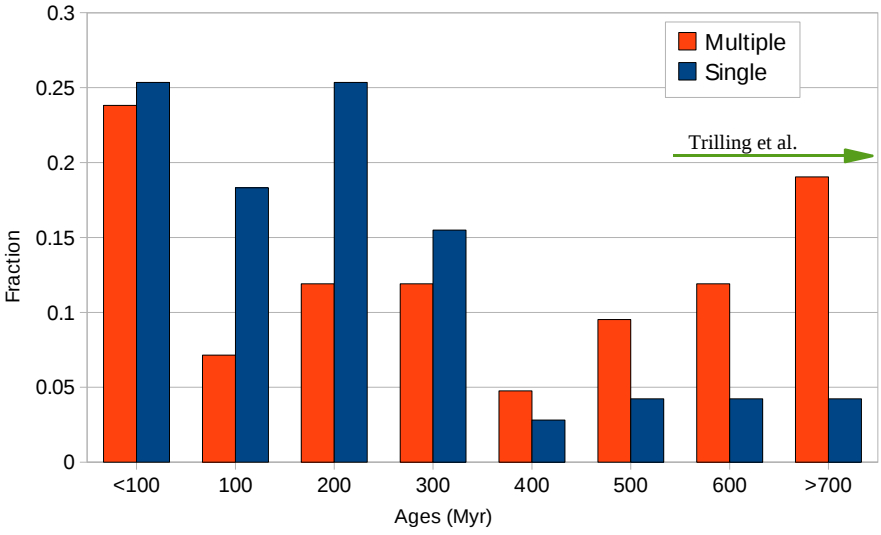

Fig. 2.— Distribution of our stellar ages separated by single/multiple. See text for more details.

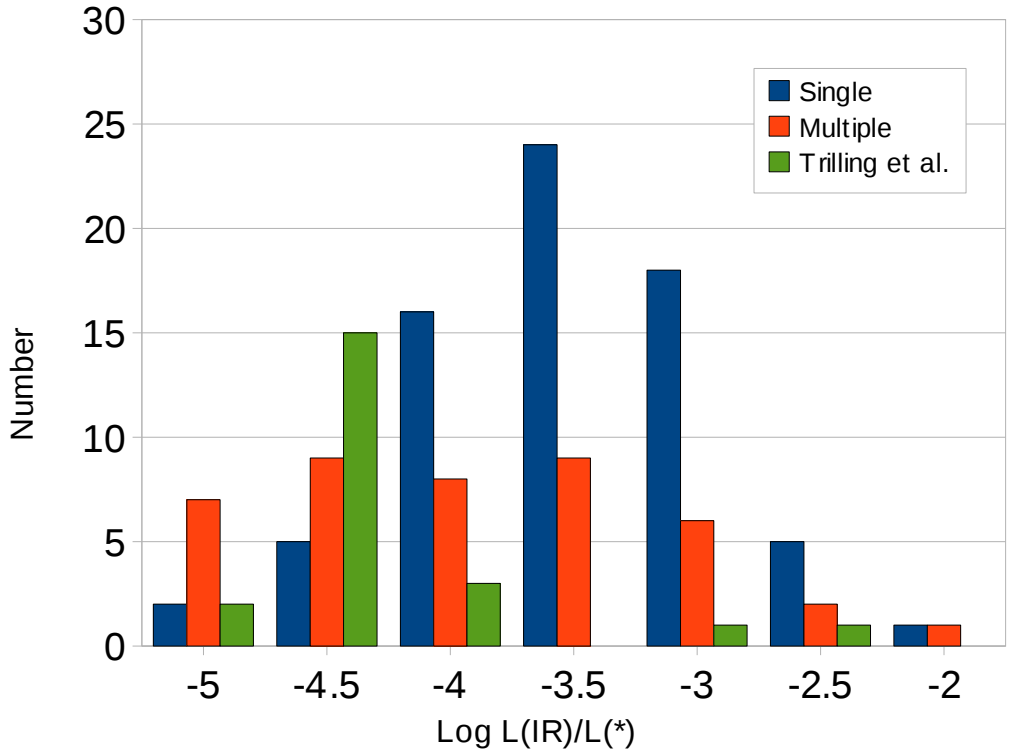

Fig. 3.— Distribution of L_{IR}/L_* for our sample broken into single and multiple stars and compared with Trilling et al. (2007) sample. Our stars tend to have higher L_{IR}/L_* compared to Trilling's which could be due to the fact that we have younger stars in our sample. Based on the KS test, these are all drawn from different distributions at the 99% significance level.

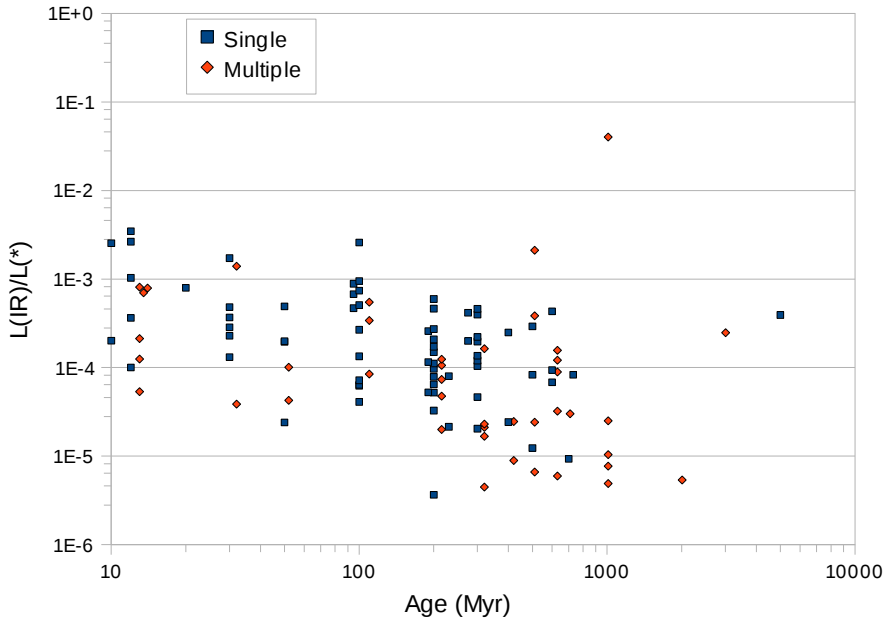

Fig. 4.— Distribution of L_{IR}/L_* for our sample as a function of age. Some points have been shifted to prevent overlap.

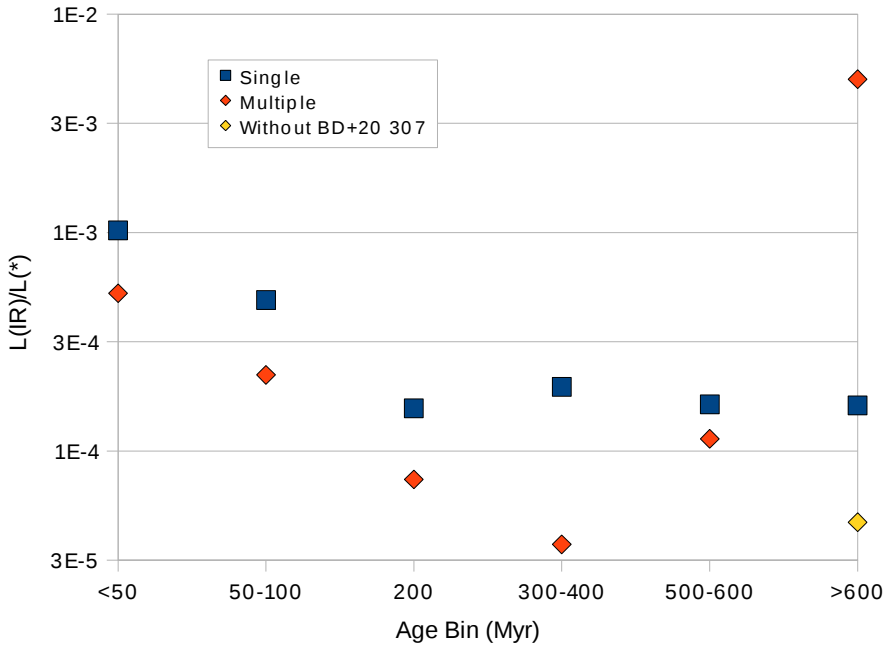

Fig. 5.— Average L_{IR}/L_* binned by age. The yellow symbol corresponds to what the average L_{IR}/L_* would be for that bin had we not included BD+20 307. See text for more details.

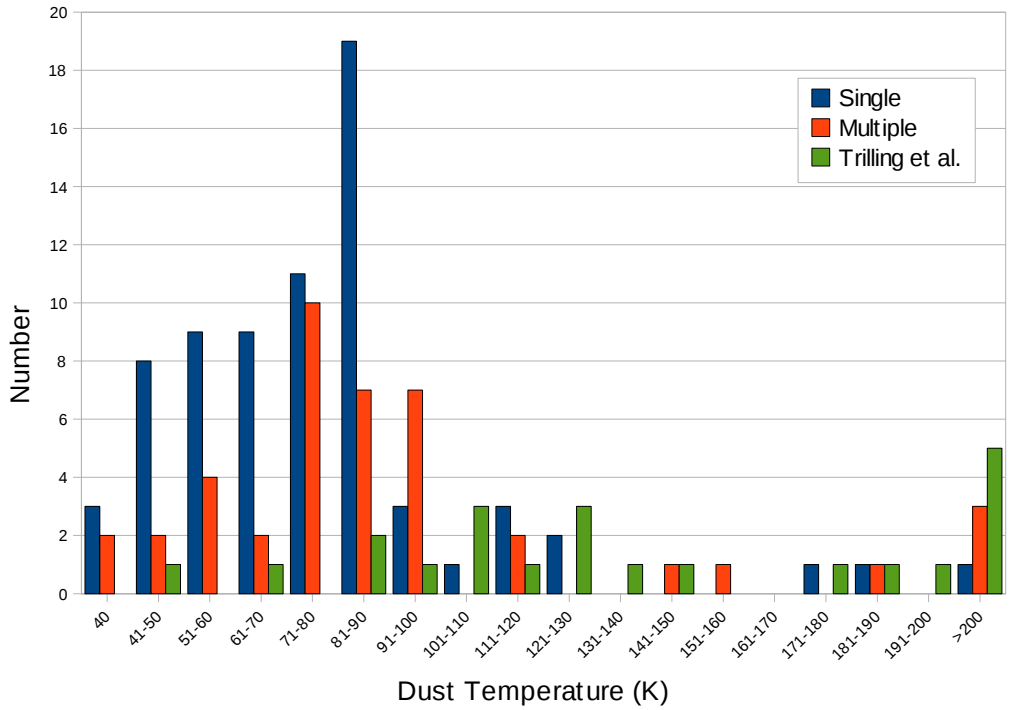

Fig. 6.— Distribution of the dust temperature for our sample and Trilling's. The large number of systems in the 81-90K bin is due to systems with only 60μm detection, where the temperature was set at 85K, as described in the text. Most of Trilling's temperatures (18/22) are upper limits since they use the upper limits to 24μm emission when they only have detections at 70μm. If they had set the blackbody fit so that its peak matches the 70μm emission, most of their sample would have temperatures of order 73K.

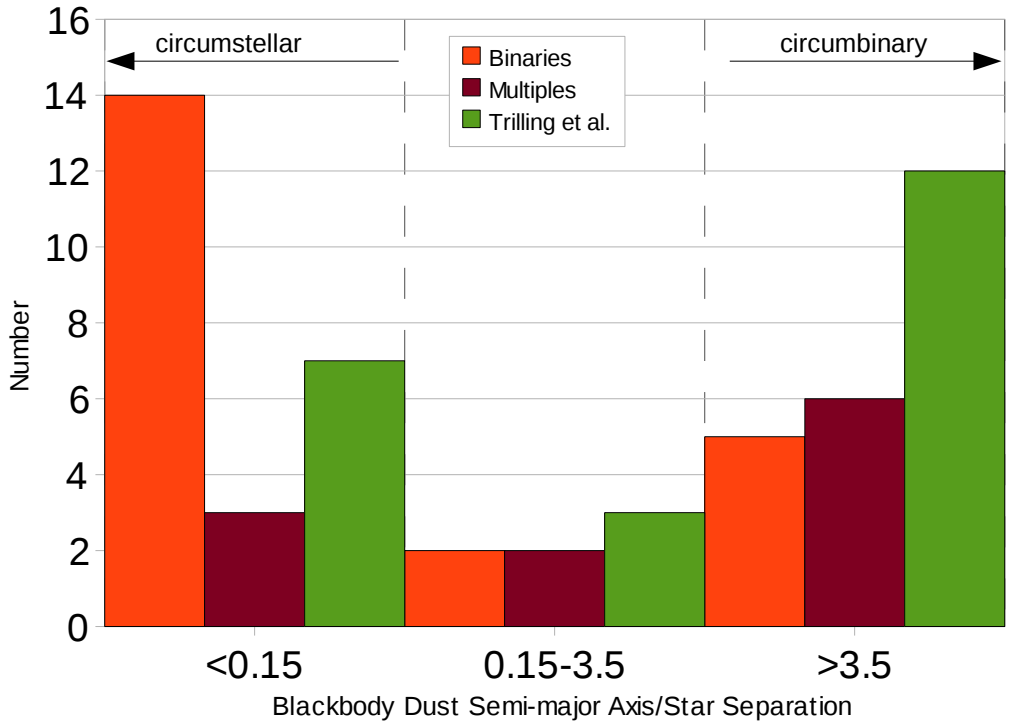

Fig. 7.— Distribution of our sample and Trilling's sample by the ratio of dust semi-major axis to binary separation. Ratios below $\sim$0.15 tend to be stable circumstellar disks while ratios higher than $\sim$3.5 tend to be stable circumbinary disks. Ratios between these two are labeled as unstable by Trilling et al. (2007). While we both have few systems in the unstable region, our sample contains more circumstellar dust than Trilling's, which contains more circumbinary systems. Our binary separations tend to be much higher than Trilling's. The purple, Multiples bar is for systems which have multiplicities greater than 2. Many of these consist of a close binary with a third star (or more) farther away. The separations used for the multiple systems is the least of all separations available.

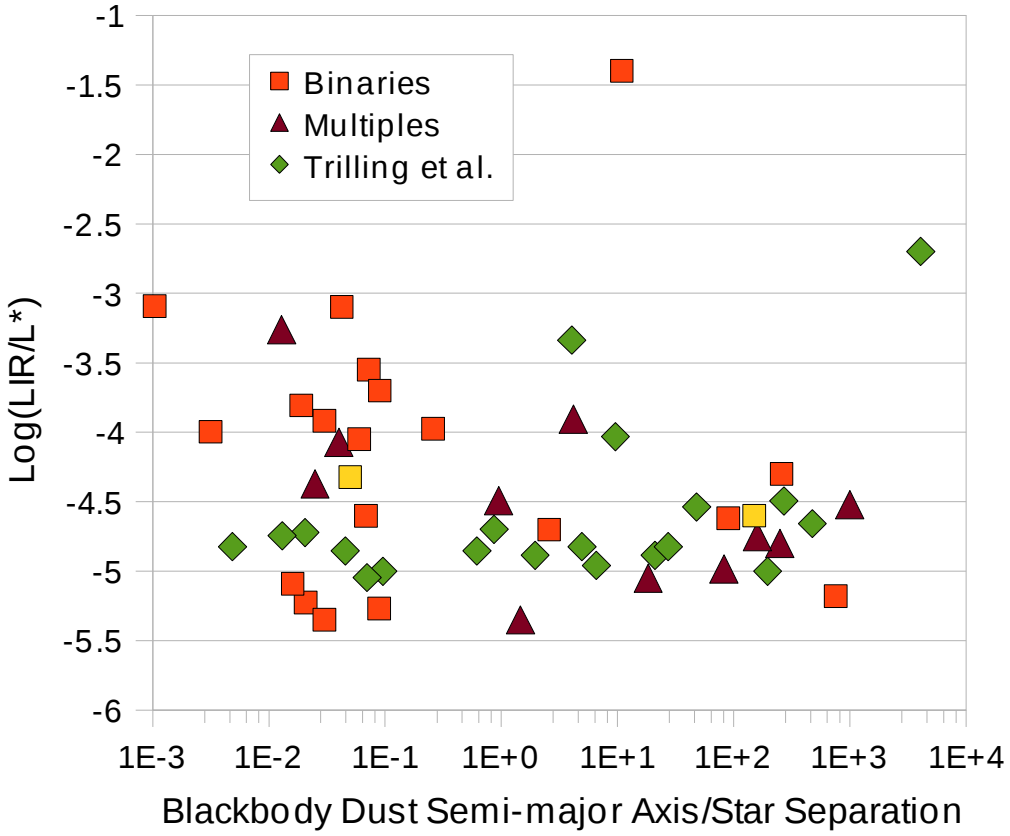

Fig. 8.— Scatter plot of our sample and Trilling's comparing the ratio of dust semi-major axis to binary separation with Log L_{IR}/L_*. The yellow symbols are the objects that overlap in both samples: HIP 15197 and HIP 66704. There is little difference between Trilling's values and ours for these two objects. All our high L_{IR}/L_* objects tend to have small ratios indicating they may be circumstellar disks. Our low L_{IR}/L_* objects tend to have a similar distribution as Trilling's sample. Trilling et al. (2007) found no trend in L_{IR}/L_* as a function of the distance ratio, but our sample appears to show that the lower ratios have a much broader spread in L_{IR}/L_* than do the higher ratios. The points have been shifted slightly to ensure that none is fully hidden. Refer to Tables 2 and 3 to see the actual values.

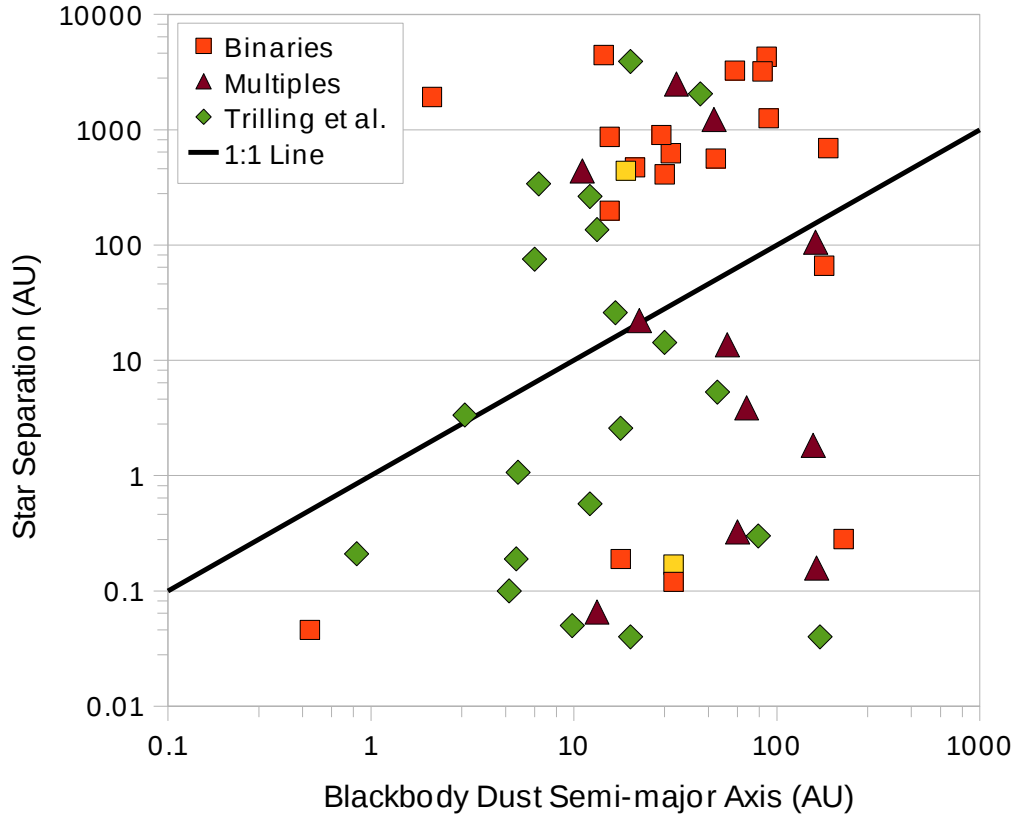

Fig. 9.— Scatter plot of the dust semi-major axis to the binary separation for both our sample and Trilling's. The yellow symbols are the two objects that overlap in both samples: HIP 15197 and HIP 66704. The black line is where the dust semi-major axis is equal to the binary separation. The points have been shifted slightly to ensure that none is fully hidden. Both samples seem fairly well distributed in dust semi-major axis. Our sample, however, appears built up mostly of wide binaries while Trilling's is mostly close binaries.

Table 1. Binary Fractions

Spectral Type	Number	Percent	From ET08	From DM91
A	14/47	30^{+7}_{-6}	46.0	
F	13/42	31^{+8}_{-6}	47.4	
G	8/12	67^{+10}_{-15}	45.0	57
K	2/5	40^{+21}_{-16}	29.1	

Note. — Our binary fractions (all as percentages) broken down by spectral type with comparison from the literature. Our errors are binomial errors estimated as described by Burgasser et al. (2003).

Table 2. Binary Star Separations

Name	Dist (pc)	Sep (″)	Dust T (K)	Dust R (AU)	L_{IR}/L_*
HIP 746	16.7	29.85	120	28	2.50E-05
HIP 6686	30.5	132.42	85	88	5.95E-06
HIP 8920	91.9	0.0005	435	0.5	4.00E-02
HIP 10679	34	13.88	100	20	8.00E-04
HIP 15197*	36.8	0.0046	95	31	2.46E-05
HIP 27072	9	96.26	90	15	7.71E-06
HIP 32480	16.5	38.02	60	29	8.93E-05
HIP 39757	19.2	29.27	85	50	5.38E-06
HIP 51658	34.3	20.18	40	179	1.06E-04
HIP 63584	37.4	119	100	18	1.01E-04
HIP 66704*	25	17.6	73	18.01	4.75E-05
HIP 68101	38.1	33	45	91	2.47E-04
HIP 71284	15.5	238.7	40	88	4.91E-06
HIP 76127	95.3	0.7	75	171	1.99E-05
HIP 76267	22.9	0.0083	190	17	2.41E-05
HIP 92024	29.2	66	320	2	8.10E-04
HIP 95261	47.7	4.17	150	15	2.13E-04
HIP 99473	88	0.0032	85	213	6.60E-06
HIP 101800	54.3	0.0027	100	31	3.86E-05
HIP 107649	15.6	55	55	27	1.21E-04
HIP 109857	25.7	127	65	62	1.56E-04

Note. — Table of our binary star separations. The two systems with asterisks are those that overlap with Trilling et al. (2007).

Table 3. Additional Star Separations

Name	Dist (pc)	Sep (″)	Dust T (K)	Dust R (AU)	L_{IR}/L_*
HIP 14576	28.5	0.002306,0.104	250	13	1.67E-05
HIP 22845	37	33.1,171.6	80	49	8.44E-05
HIP 35550	18	0.215,6.975	60	71	8.93E-06
HIP 42430	19.9	1.11,93.46	80	21	3.21E-05
HIP 48164	89.5	27.8,32.7	85	32	5.48E-04
HIP 57632	11.1	39.7,79.5	160	11	4.25E-05
HIP 70090	75.8	0.0043,36	120	64	2.11E-05
HIP 71075	26.1	0.07,31.6	55	151	1.04E-05
HIP 81126	92.7	0.0017, 0.068, 0.11	80	157	3.01E-05
HIP 81641	92.9	0.147,69.72	95	57	1.24E-04
HIP 90185	44.3	2.39,36.1	100	155	4.46E-06
		Uknown Separation			
HIP 11437	42.3		65	10	7.90E-04
HIP 19893	20.3		80	31	2.30E-05
HIP 25486	26.8		73	18.93	5.34E-05
HIP 32775	33.2		45	68	1.63E-04
HIP 64921	85.4		80	39	3.39E-04
HIP 69682	61.3		85	10	2.11E-03
HIP 70344	70.1		85	26	3.85E-04
HIP 92680	49.7		73	15.77	1.25E-04
HIP 99273	53.5		95	15	1.39E-03
HIP 108809	30.1		75	18	7.33E-05

Note. — Table of our multiple star separations and those where we have not obtained separations in the literature. For the multiple stars we have only used the smallest separation in order to compute the separation in AU and the ratio of dust to star separation.